

# Coarsening dynamics at unstable crystal surfaces

Paolo Politi<sup>1</sup>

<sup>1</sup>*Istituto dei Sistemi Complessi, Consiglio Nazionale delle Ricerche,  
via Madonna del Piano 10, 50019 Sesto Fiorentino (Italy)  
paolo.politi@cnr.it*

In this paper we focus on crystal surfaces led out of equilibrium by a growth or erosion process. As a consequence of that the surface may undergo morphological instabilities and develop a distinct structure: undulations, mounds or pyramids, bunches of steps, ripples. The typical size of the emergent pattern may be fixed or it may increase in time through a coarsening process which in turn may last forever or it may be interrupted at some relevant length scale. We study dynamics in three different cases, stressing the main physical ingredients and the main features of coarsening: a kinetic instability, an energetic instability, and an athermal instability.

## I. PREAMBLE

This paper appears in a special issue of *Comptes Rendus Physique* devoted to coarsening dynamics. My contribution focuses on coarsening processes occurring at the surface of a crystal as a result of an instability. The meaning of coarsening in this context is clearly exemplified by the images (a1-a6) in Fig. 1. Here we provide Scanning Tunneling Microscope (STM) images of a growing Cu/Cu(100) surface at different times (the number of deposited monolayers (ML) is proportional to time and it is indicated on the bottom right of each image). As you can see, the crystal surface does not grow flat and it develops a clear mound structure whose typical size increases in time. Images (c1-c4) in the same figure refer to a similar growth process of Pt/Pt(111). In this case coarsening stops after a while.

There are so many unstable growth processes at a crystal surface that it is not possible to cover all them in this short review. For this reason I will treat a personal shortlist of phenomena. Also, I will not try to report all relevant bibliography, because I am more interested to develop general considerations and to highlight some aspects.

I have chosen three main topics with different features: i) The kinetic instability of a growing high symmetry surface. It takes place because the growth process is too fast and the surface cannot relax to its equilibrium shape (a flat surface in this case). ii) The energetic instability of a surface in heteroepitaxy. Here, dynamics is driven by the minimization of the system free energy. iii) The nonthermal instability of a surface under ion beam erosion. In this case surface morphology changes under the action of an incident beam of energetic ions.

The first topic on the kinetic instability, which is introduced in Sec. II and discussed in Sec. III, is the most extended one because it has long been studied in *specific* relation to coarsening. In fact, experimental studies of this phenomenon show all possible scenarios. Here above we have already mentioned perpetual coarsening and interrupted coarsening. The former, illustrated in Fig. 1(a1-a6), means that the size of the emergent pattern increases in time forever. The latter, shown in Fig. 1(c1-c4), means that coarsening stops when the size reaches some special length scale, not depending on boundary conditions. Finally, it is also possible that the size of the pattern keeps constant in time (no coarsening). This case is shown in images (b1-b2) of Fig. 1, where atomic steps of a growing Cu surface meander with a typical lengthscale which does not grow in time.

It may seem amazing we mention “no coarsening” as a coarsening scenario, but all these scenarios can be understood within the same picture and model. This remark also allows to introduce a second, important reason for which topic (i) is discussed more widely: we have a much deeper theoretical comprehension of its coarsening behaviour than for other topics. This is possible because the scientific community has agreed on the special relevance of given growth equations and many studies have been devoted to them.

In Sec. IV we discuss an energetic instability occurring in heteroepitaxy. In this case we can imagine to deposit a semiconductor (e.g., Ge) on top of a different one (e.g., Si). Since the two elements have different lattice constants, the adsorbate must squeeze or stretch in order to grow coherently with the substrate. This fact leads to an accumulation of elastic energy which then must be released. A possible way out is a phenomenon with relevant applications: the formation of quantum dots through a self-organized growth process. This is illustrated in images (d1-d4) of Fig. 1, where a suitable combination of Si and Ge is deposited on top of Si(100). In this case the source of the instability is the minimization of the elastic energy, whose nonlocal character makes much more involved a theoretical description. It is not surprising that there is no simple equation able to describe the main features of the dynamics.

Finally, in Sec. V we study an athermal instability, due to the erosion of a crystal surface with an incident flux of high energy ions. The resulting morphology is shown in images (e1-e4) of Fig. 1 for the case of Si(001) under the exposure to  $\text{Kr}^+$ . In ion beam erosion the elementary process changing surface morphology is the ejection of surface atoms because of the impact of a high energy ion. This process is not thermally activated, as opposed to surface

processes driving the dynamics of the systems in topics (i) and (ii). Theoretical descriptions of the evolution of a surface under ion beam erosion are very phenomenological and the experimental picture does not seem to be entirely clear.

I hope both people working and not working in this field find something useful. The non specialist should understand the basic physical ingredients of the phenomena we are going to discuss and get a general idea of them. The specialist might find of some interest the focus on coarsening in different contexts. Some aspects of an unstable crystal surface closely resemble phase separation while other aspects fall into the category of pattern formation. For this reason the reader may find some connections with the contributions by Leticia Cugliandolo and by Alexander A. Nepomnyashchy in this issue.

## II. THE PHYSICAL PICTURE

A crystal surface at thermal equilibrium undergoes the well known roughening transition, according to which above the temperature  $T = T_R$  the system is characterized by diverging height fluctuations. Below  $T_R$  a crystal surface is characterized by orientations of minimal free energy. Therefore, quenching the system to  $T < T_R$ , an unstable surface splits into regions of different orientations (facets) whose size increases in time through a process of phase separation where the local slope is the order parameter [1, 2]. In the following we are not dealing with such process, but we are mostly speaking about thermal systems which are kept out of equilibrium by a flux of atoms.

Surface dynamics has two special features with respect to bulk dynamics: it can be more easily imaged and it is faster. The former feature is trivial. The latter is due to the fewer number of neighbouring atoms, which makes thermally activated processes more likely. The ensemble of atomistic processes occurring at a crystal surface is schematically depicted in Fig. 2, where two main objects stand out, steps and adatoms. Adatoms (adsorbed atoms) are provided by the incoming flux and by thermal detachment from steps. They diffuse until they (re)attach to steps or go (back) to the vapour phase. If the surface is cut along a high symmetry orientation, e.g. the orientation (100) of a cubic crystal, the perfect surface does not contain steps, which are created by the nucleation and aggregation processes, when adatoms stick together. Conversely, if the surface is not cut along a high symmetry orientation, then steps are naturally present.

The key point is that step dynamics is usually much slower than adatom dynamics. This may be a drawback for atomistic simulations but it is useful for analytical treatments. In fact, simulating a system where very different time scales are relevant is problematic. On the other hand, different time scales may allow to adopt quasi static approximations, where the dynamics of certain (fast) variables is *slaved* to the instantaneous value of other (slow) variables. In practice, adatom diffusion can be studied assuming steps are fixed, then step motion is determined via the average diffusion current attaching to or detaching from steps.

The true origin of thermal instabilities we are going to discuss is the existence of an asymmetric diffusion current between steps, which may be preexisting (not high symmetry surface) or be created by the dynamics itself (high symmetry surface). Such net current can have an intrinsic or an extrinsic origin. Surface reconstruction, asymmetry in step attachment/detachment rates ( $K' \neq K''$  in Fig. 2), and step-step interaction are intrinsic motivations. Impurities and an applied electric current are among extrinsic motivations. Let us explain with a simple one-dimensional model why a current asymmetry may produce an instability, see Fig. 3a.

The speed of a step depends on the net balance between attaching and detaching adatoms. It is useful to separate the balance of exchanging atoms with the upper terrace,  $f_+$ , from the balance of exchanging atoms with the lower terrace,  $f_-$ , because a net current  $J$  appears when they are different:  $J(\ell) = f_-(\ell) - f_+(\ell)$ . Each contribution depends on the size  $\ell$  of the terrace, of course. Making reference to Fig. 3a, we can write

$$\dot{x}_n = f_+(\ell_n) + f_-(\ell_{n-1}) \quad \text{and} \quad \dot{\ell}_n = \dot{x}_{n+1} - \dot{x}_n. \quad (1)$$

It is useful to separate contributions in a symmetric ( $s(\ell)$ ) and an antisymmetric ( $a(\ell)$ ) part,

$$f_{\pm}(\ell) = s(\ell) \pm a(\ell), \quad (2)$$

so that  $J(\ell) = f_-(\ell) - f_+(\ell) = -2a(\ell)$ . Replacing in Eq. (1) we get

$$\dot{\ell}_n = [s(\ell_{n+1}) - s(\ell_{n-1})] + [a(\ell_{n+1}) + a(\ell_{n-1}) - 2a(\ell_n)], \quad (3)$$

which immediately clarifies the different role of the two parts, the symmetric one entering with a first derivative, the antisymmetric one entering via a second derivative. We can now perform a linear stability analysis of the uniform train of steps, writing

$$\ell_n(t) = \ell + \epsilon_n(t) = \ell + \epsilon_0 \exp(iqn + \sigma t) \quad (4)$$

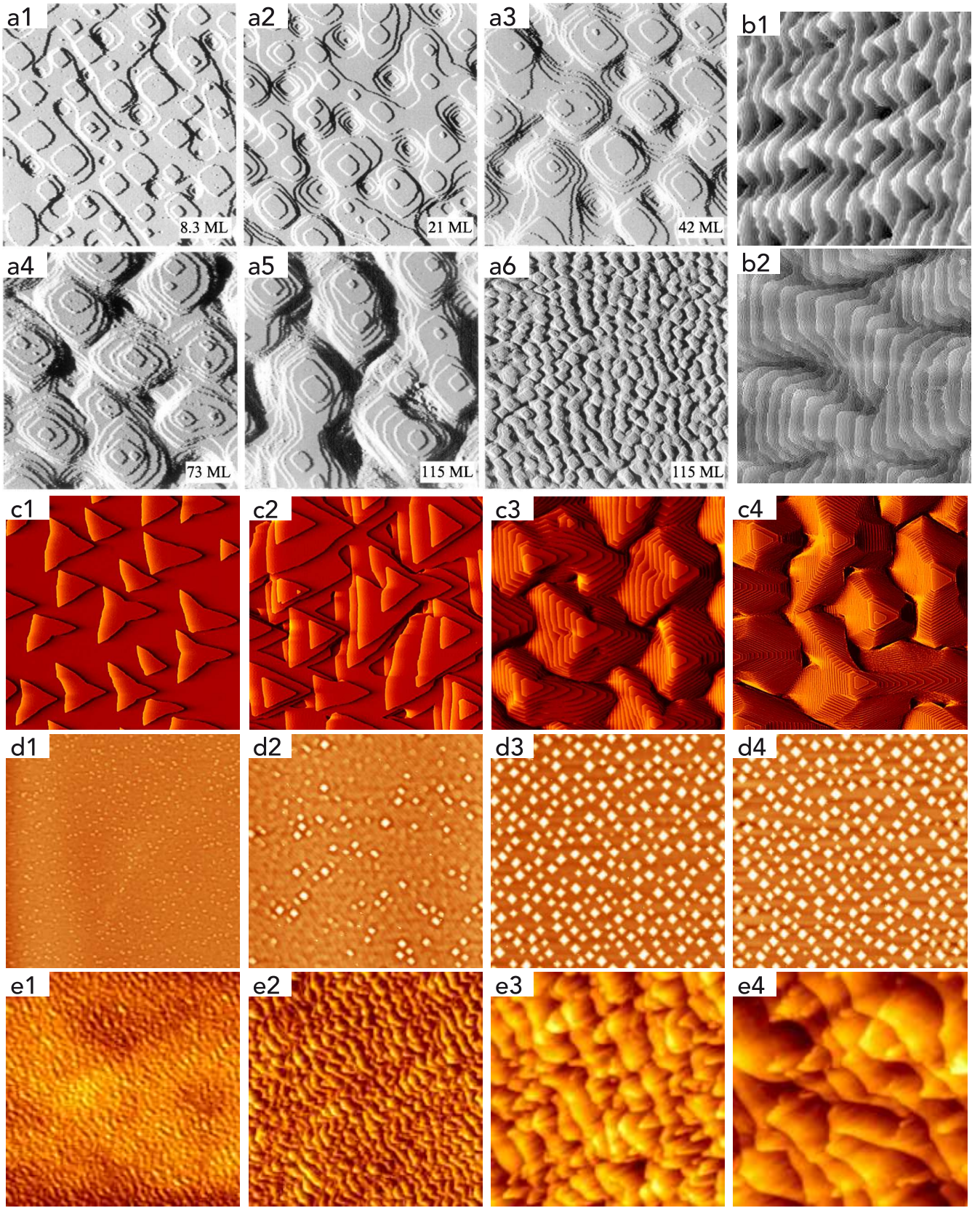


FIG. 1: (a1-a6) STM images of Cu/Cu(100) at various thicknesses. The area is  $1000 \times 1000 \text{ \AA}$  (a6 is  $5000 \times 5000 \text{ \AA}$ ). Taken from Ref. [3]. (b1-b2) STM images of (b1) Cu(0 2 24) and (b2) Cu(1 1 17). The area is  $40 \times 40 \text{ nm}$ . Taken from Ref. [4]. (c1-c4) STM images of Pt/Pt(111) at (c1) 0.35 ML, (c2) 3 ML, (c3) 12 ML, (c4) 90 ML. The area is  $2900 \times 2900 \text{ \AA}$ . Taken from Ref. [5]. (d1-d4) AFM images of Si<sub>0.75</sub>Ge<sub>0.25</sub>/Si(100) (d1) as grown, (d2) after 1.5h of annealing, (d3) after 18h of annealing, and (d4) after 54h of annealing. The area is  $5 \times 5 \mu\text{m}^2$ , the vertical scale is 25nm. Courtesy of Isabelle Berbezier. (e1-e4) STM images of Si(001) after 2 keV Kr<sup>+</sup> ion exposure and ion fluences of (e1)  $10^{20}$ , (e2)  $3 \times 10^{20}$ , (e3)  $10^{21}$ , (e4)  $3 \times 10^{21} \text{ ions/m}^2$ . Taken from Ref. [6].



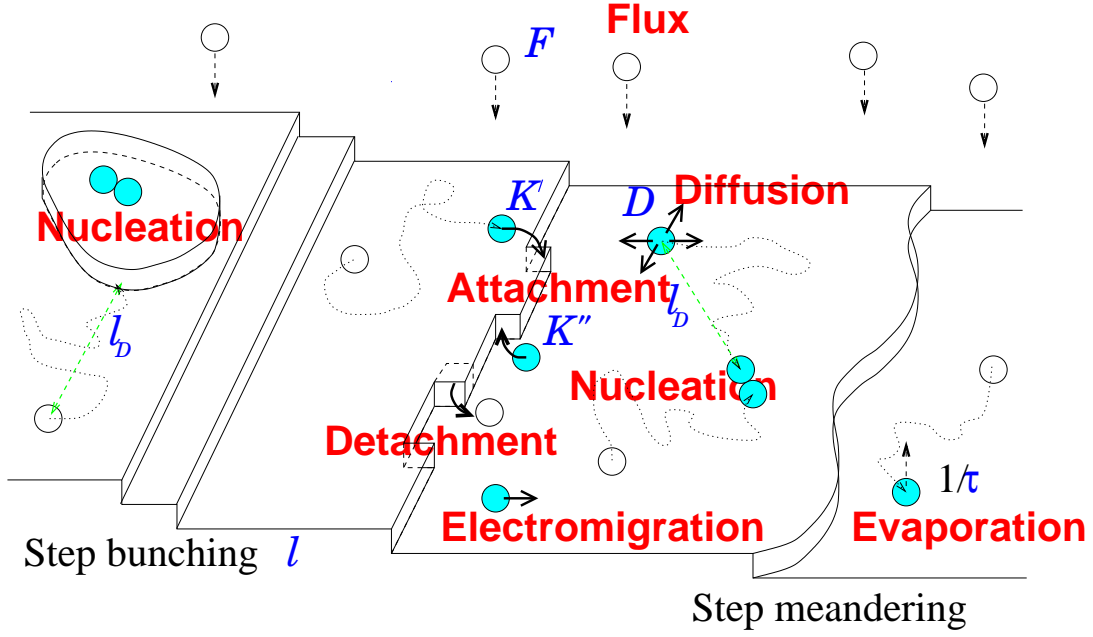


FIG. 2: Schematics of basic elementary processes occurring at a crystal surface. Adatoms (empty circles) are provided by the incoming flux (at rate  $F$ ) and by detachment from steps. Once an adatom is on a terrace, it may diffuse (at rate  $D$ ), it may evaporate (at rate  $\tau^{-1}$ ), it may attach to a step (at rates  $K', K''$ ) or it may encounter another adatom and nucleate a new terrace. Steps may be preexisting (long straight or meandering steps) or may be created by nucleation (step encircling the nucleated island). Two lengths are specially important during growth: the distance  $\ell$  between preexisting steps and the diffusion length  $\ell_D$ , i.e. the distance traveled by an adatom before nucleating a new terrace or being incorporated in a terrace. If  $\ell \gg \ell_D$ , the surface behaves as a high symmetry surface and preexisting steps play no role. In the opposite limit,  $\ell \ll \ell_D$ , dynamics is dominated by step-flow growth and nucleation of new terrace is absent. Three main instabilities may occur: step-bunching (a train of equally spaced steps is unstable against fluctuations of their distance); step-meanderings (a straight step is unstable); mound formation (islands are nucleated at a rate larger than their coalescence, so that the flat surface is unstable).

where a positive real part of  $\sigma(q)$  signals an instability. Replacing Eq. (4) in (3) we finally obtain

$$\sigma(q) = (1 - \cos q)J'(\ell) + i(2s'(\ell)\sin q), \quad (5)$$

so that

$$\text{instability} \longleftrightarrow J'(\ell) > 0. \quad (6)$$

Strictly speaking, this analysis is valid for a surface looking like a staircase, where all steps are of the same type: ascending or descending steps. This is the case of images (b1-b2) in Fig. 1, which represent a *vicinal* surface of copper.[49] The nucleation and aggregation processes determine ascending and descending steps, producing a morphology like the one you can see in Figs. 1(a1-a6) and Figs. 1(c1-c4). In this case steps are continuously created and destroyed and a mesoscopic continuum description, in terms of the local height  $z(\mathbf{x}, t)$ , is preferable. This is the approach used in the next Section.

### III. HIGH SYMMETRY ORIENTATIONS

In very general terms, the local velocity of the surface,  $\partial_t z(\mathbf{x}, t)$ , is a function of the surface profile. If we neglect long-range forces (essentially elasticity, in this context) such dependence is limited to  $z(\mathbf{x}, t)$  and to spatial derivatives of various order. In the case the deposited material is the same of the substrate (homoepitaxial growth), translational invariance in the growth direction does not allow for an explicit dependence on  $z$ . Finally, if desorption is negligible dynamics “reduces” to an ensemble of surface processes which conserve matter. Therefore, if  $z(\mathbf{x}, t)$  is the local height with respect to the average height of the surface, its time derivative must satisfy the continuity equation,

$$\partial_t z(\mathbf{x}, t) = -\nabla \cdot \mathbf{j}(\nabla z, \nabla^2 z, \dots). \quad (7)$$

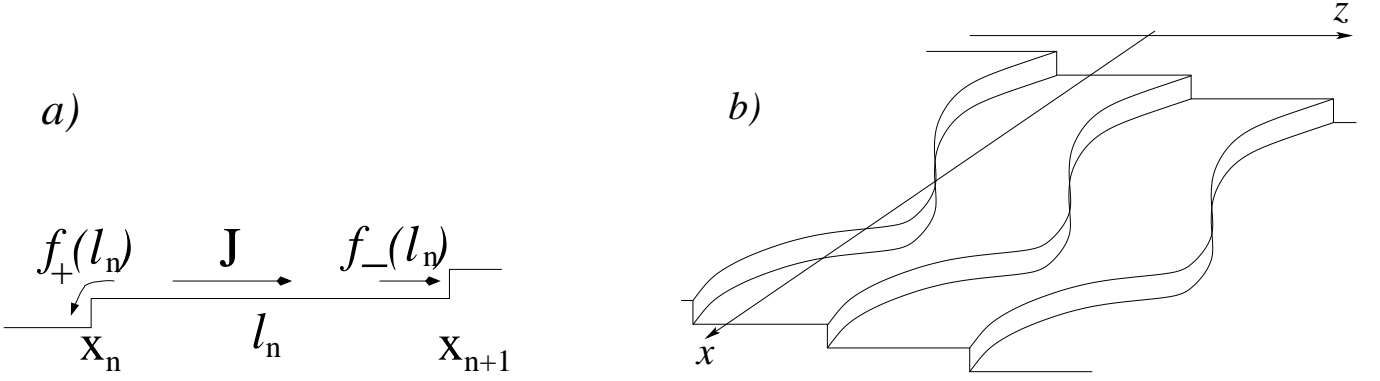


FIG. 3: a) Adatoms may attach to or detach from the upper and lower step. The quantity  $f_+(\ell)$  ( $f_-(\ell)$ ) represent the net balance of the exchange of adatoms between a step and the upper (lower) terrace of size  $\ell$ . A positive  $f_{\pm}$  means that more adatoms attach than detach. The current  $J$  is defined as  $J = f_-(\ell) - f_+(\ell)$ . b) A train of equally spaced steps which meander in phase. This type of instability allows to reduce 2D step dynamics to an effective 1D model for the variable  $z(x, t)$ .

The rest of this Section will be devoted to introduce a couple of relevant equations, one in  $D = 1$  and one in  $D = 2$ , and to discuss what we know about them. The case 1D, simpler than the case 2D, will also serve to introduce some concepts.

#### A. $D = 1$

We can rightly ask if  $D = 1$  has any experimental relevance. The answer is positive because a 2D vicinal surface may form an effective 1D pattern, when steps meander in-phase while preserving their distance: see Fig. 1(b1) for a clear experimental realization and Fig. 3b for its theoretical modelization. If this is the case, a rigorous analysis [7, 8] has proved that the resulting step dynamics can be described by an effective one-dimensional equation. Therefore, the 1D version of Eq. (7) describes the dynamics of a vicinal surface if its steps synchronize along a high symmetry orientation.

According to a fairly general model [7] which includes elastic interactions among steps,[50] the evolution of an in-phase train of steps is ruled by the equation

$$\partial_t z = -\partial_x \{B(m) + G(m)\partial_x [C(m)\partial_x m]\}. \quad (8)$$

If we change variable, defining

$$u = \int_0^m ds C(s) \quad (9)$$

the evolution of  $u$  satisfies

$$\partial_t u = -C(u)\partial_{xx} [B(u) + G(u)u_{xx}], \quad (10)$$

which looks like a generalized Cahn-Hilliard (CH) equation. In fact, the standard CH eq. is obtained if  $C(u)$  and  $G(u)$  are positive constants and  $B(u) = c_1 u - c_2 u^3$ , with  $c_{1,2} > 0$ . Its generalization, however, should preserve the linear stability analysis of the trivial solution  $u \equiv 0$ , which corresponds to say the functions  $B, G, C$  have a fixed form for small  $u$ ,

$$B(u) \simeq c_1 u, \quad G(u) \simeq c_3, \quad C(u) \simeq c_4, \quad (11)$$

with all  $c_i > 0$ . Given these relations,  $u$  and  $m$  are just proportional for small slope,  $u \simeq c_4 m$ . Furthermore, if we assume  $u(x, t) = u_0 e^{\sigma t + i q x}$  in the limit  $u_0 \rightarrow 0$  we get

$$\sigma(q) = c_1 c_4 q^2 - c_3 c_4 q^4, \quad (12)$$

which is the linear spectrum for the (generalized) CH equation.

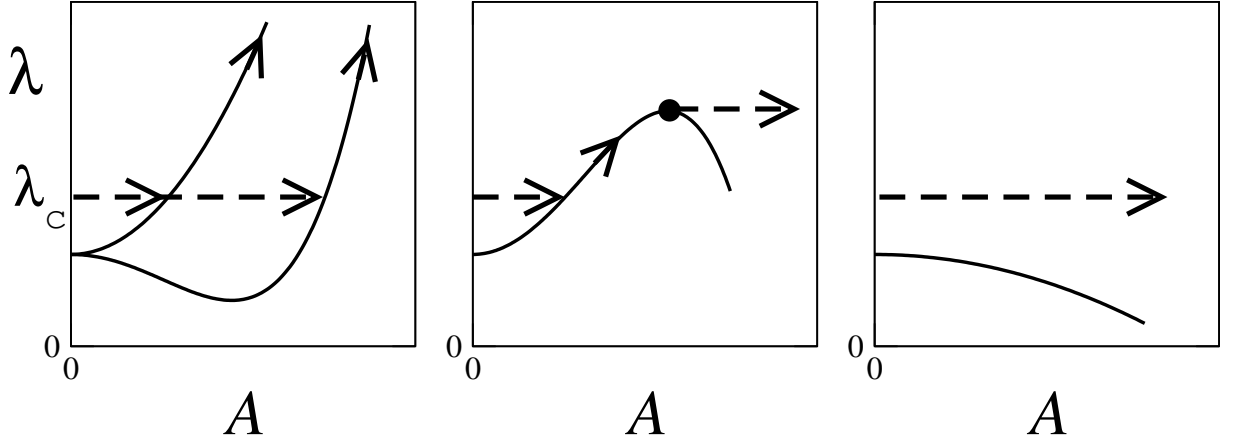


FIG. 4: Scenarios of perpetual (left), interrupted (centre), and no coarsening (right). In all cases  $\lambda(A \rightarrow 0) = \lambda_0$  is the minimal unstable wavelength when studying the linear stability of the flat profile  $u = 0$ . More precisely, if  $\sigma(q) = c_1 c_4 q^2 - c_3 c_4 q^4$  is the linear spectrum (see Eq. (12)) then  $\sigma(2\pi/\lambda_0) = 0$ . All wavelengths larger than  $\lambda_0$  are unstable and  $\lambda_c = \sqrt{2}\lambda_0$  is the most unstable one, since  $\sigma'(2\pi/\lambda_c) = 0$ . Arrows indicate dynamics in a qualitative way. Arrows ending dashed lines mean the pattern has a constant wavelength and an increasing amplitude: this may occur either in the linear regime (short times, small  $A$ ) or at large times. Arrows along a  $\lambda(A)$  curve mean coarsening.

The key point of our analysis is to study coarsening as a long-wave instability [9] of periodic steady states. This means that a periodic configuration may be unstable under large scale fluctuations of the wavelength. In the case of Eq. (10), if we require that the constant average spatial value of the order parameter vanishes,  $\langle u \rangle = 0$  (which corresponds to say the step has a high symmetry orientation) periodic steady states are given by the vanishing of the quantity in square brackets, i.e.  $u_{xx} = -B(u)/G(u)$ . Therefore, steady states correspond to the oscillations of a fictitious particle in the potential  $V(u) = \int du B(u)/G(u)$ , which has the parabolic form  $V(u) \simeq (c_1/2c_3)u^2$  for small  $u$ , i.e. for small  $m$ . We leave out all technical details which can be found elsewhere [10] and focus on the spirit of the analytical treatment and, of course, on the main results.

We need to study how a periodic steady state  $u_\lambda(x)$  responds to a weak spatial perturbation. Because of translational invariance, also  $u_\lambda(x + \Phi)$  is a good steady state and if the phase  $\Phi$  acquires a slow spatial dependence, the temporal response is slow as well. Formally, this amounts to assume that  $\Phi = \Phi(X, T)$ , where  $X = \epsilon x$  and  $T = \epsilon^2 t$  are slow variables and the different dependence on  $\epsilon$  is attributable to the expected diffusive character of the phase. The introduction of these new variables allows us to perform a perturbative multiscale analysis, which finally provides an equation describing the dynamics through the diffusion equation  $\partial_T \Phi = D \partial_{XX} \Phi$ , where the phase diffusion coefficient  $D$  can be explicitly derived and be shown to have the form

$$D = -D_0(A) \left( \frac{\partial \lambda}{\partial A} \right)^{-1}. \quad (13)$$

Here above  $A$  and  $\lambda$  are the amplitude and the wavelength of the steady states. The quantity  $\lambda$  (corresponding to the period of oscillation in the potential  $V(u)$ ) is itself a function of  $A$ . Since  $D_0 > 0$ , a phase instability ( $D < 0$ ) is present if and only if  $\lambda$  is an increasing function of  $A$ . Therefore, we have a pretty simple criterion to discriminate among different scenarios, see Fig. 4: perpetual coarsening (increasing  $\lambda(A)$  or  $\lambda(A)$  has a minimum), interrupted coarsening ( $\lambda(A)$  has a maximum), and no coarsening (decreasing  $\lambda(A)$ ). In fact, we have even more than that, because the knowledge of  $D(\lambda)$  allows to determine the coarsening law  $\lambda(t)$  at large space and time scales. In this regime the only relevant time scale is time  $t$  and the only relevant spatial scale is the wavelength  $\lambda$  of the structure, so that

$$|D(\lambda)| \approx \frac{\lambda^2}{t}. \quad (14)$$

Using this relation and evaluating the asymptotic profile of steady states it is possible to derive the coarsening exponent,  $\lambda(t) \approx t^n$ . Using the explicit expressions of functions  $B(u)$ ,  $C(u)$ , and  $G(u)$  we can find when perpetual coarsening occurs and what is the coarsening exponent.

In practice, we have found that coarsening is switched on by elastic interaction and  $n = 1/4$  or  $n = 1/6$ , depending what type of adatom diffusion is more efficient to relax the surface:  $n = 1/4$  if adatoms mainly diffuse along the steps

and  $n = 1/6$  if they diffuse mainly on terraces. We should also add that the criterion of a maximum of  $\lambda(A)$  signaling interrupted coarsening is able to explain the role of anisotropy [11], which has precisely this effect. The theory has proved to be extremely powerful. Unfortunately, from an experimental point of view we are not aware of meandering systems producing coarsening during all the experimental observation time: either coarsening is absent or it lasts very little.

## B. $D = 2$

Real two-dimensional, high-symmetry surfaces growing under slow deposition have been well studied and coarsening is a common dynamical scenario, see Figs. 1a,c. However, we should start by saying that a quantitative comparison with experiments can be difficult because attaining the asymptotic regime for enough time to allow the extraction of the coarsening exponent  $n$  from a log-log plot of  $L$  (the size of the emergent structure) vs  $t$  is very hard. In this respect we can observe that an exponent  $n \leq 1/3$  requires to increase time by at least a factor  $10^3$  to increase  $L$  by a factor 10, and this may not be feasible.

Performing a phase stability analysis in two spatial dimensions is by far more complicated than in  $D = 1$ , because a periodic structure is now defined by two wavevectors, so two phases  $\Phi_1, \Phi_2$  appear, each one depending on both spatial coordinates,  $X_1, X_2$ . Therefore a diffusive behavior is now described by a system of equations,

$$\partial_T \Phi_i = \sum_{j,k,\ell} D_{k\ell}^{ij} \partial_{X_k X_\ell} \Phi_j \quad (15)$$

which in principle means 12 different coefficients, even if the symmetries of the pattern may strongly reduce such number.

Our analysis has focused on the following class of equations,

$$\frac{\partial h(\mathbf{x}, t)}{\partial t} = -\nabla \cdot [\mathbf{j}(\nabla h) + \nabla(\nabla^2 h)]. \quad (16)$$

If the current  $\mathbf{j}$  is derivable from a potential, i.e.  $\mathbf{j} = -\nabla_{\mathbf{m}} V(\mathbf{m})$ , then taking the gradient of left and right hand sides of Eq. (16), the equation seems to reduce to a standard phase separation process,

$$\frac{\partial \mathbf{m}}{\partial t} = -\nabla \cdot \{ \nabla \cdot [\nabla^2 \mathbf{m} - \nabla_{\mathbf{m}} V(\mathbf{m})] \}. \quad (17)$$

However, this similarity is only apparent. Firstly, on the right hand side we have  $\nabla \nabla$  rather than  $\nabla^2$ :  $\nabla \nabla$  means to take the gradient of the divergence, while  $\nabla^2$  means to take the Laplacian of each separate component. Secondly,  $\mathbf{m}$  is a *constrained* order parameter, because  $\nabla \times \mathbf{m} = \nabla \times \nabla h \equiv 0$ . This constraint is related to the domain wall straightness: if the slope is the order parameter two regions of constant, different slopes  $\mathbf{m}_1, \mathbf{m}_2$ , must forcibly cross along a straight line, so domain walls are straight, which is not the case in standard phase separation processes. It is worth stressing that both remarks do *not* apply in  $D = 1$ , where crystal growth and phase separation do have strong similarities, as evidenced by the generalized CH equation (10).

In  $D = 2$  instead, crystal growth dynamics as given by Eq. (16) are genuine new dynamics. We refer to papers [12, 13] for details and for a thorough discussion of the relevant bibliography. Here we report the main results focusing on the coarsening exponents for models providing a perpetual coarsening scenario.[51] While the symmetry of the pattern does not seem to be a relevant feature, the key point is the long time behavior of the slope in “facets”, which can either be constant (both in space and time) or can tend to increase in time. This property can be established a priori via a simple inspection of the current  $\mathbf{j}(\mathbf{m})$ , which can vanish for  $\mathbf{m} = 0$  only or also for some finite values  $\mathbf{m}_i^*$ , called magic slopes and related by suitable rotational symmetry operations. If  $\mathbf{j} = -\nabla_{\mathbf{m}} V(\mathbf{m})$ , these slopes are the minima of the potential. According to our results, two main universality classes exist, depending on the presence or the absence of magic slopes: in the former case (faceting),  $n = 1/3$  while in the latter case (increasing slope),  $n = 1/4$ .

In the literature there have been several heuristic derivation of coarsening exponents for crystal growth. Here we report a simple explanation of the exponent  $n = 1/3$  in the case of faceting, proposed by Golubović et al. in Ref. [14]. Two hypotheses are used in such derivation, the first being the existence of one single length scale, the wavelength of the periodic pattern. The second hypothesis is that our model, Eq. (16), can be rewritten in the variational form  $\partial_t h = -\delta \mathcal{F} / \delta h$ , where  $\mathcal{F} = \int d\mathbf{x} [\frac{1}{2} \mathbf{m}^2 + V(\mathbf{m})]$ . Within these hypotheses, the excess free energy is concentrated along domain walls, where the slope varies from a minimum of  $V(\mathbf{m})$  to another minimum, so  $\mathcal{F} = \sigma_{\text{DW}} \mathcal{L}$ , where  $\sigma_{\text{DW}}$  is the domain wall (DW) energy cost per unit length and  $\mathcal{L}$  is the total length of domain walls. If  $\lambda$  is the average size of

domains, there will be a DW length of order  $\lambda$  in a region of order  $\lambda^2$ , so  $\mathcal{F}/\mathcal{A}_s \approx \sigma_{\text{DW}}/\lambda$ , where  $\mathcal{A}_s$  is just the total surface area. From the variational form of the evolution equation we can easily write that

$$\frac{1}{\mathcal{A}_s} \frac{d\mathcal{F}}{dt} = \frac{1}{\mathcal{A}_s} \int d\mathbf{x} \frac{\delta\mathcal{F}}{\delta h} \frac{\partial h}{\partial t} = -\frac{1}{\mathcal{A}_s} \int d\mathbf{x} \left( \frac{\partial h}{\partial t} \right)^2 = -\langle (\partial_t h)^2 \rangle. \quad (18)$$

Because of faceting the height of the structure scales as  $\lambda$ , so that  $\langle (\partial_t h)^2 \rangle \approx (\partial_t \lambda)^2$  and finally

$$-(\partial_t \lambda)^2 \approx \frac{1}{\mathcal{A}_s} \frac{d\mathcal{F}}{dt} = \frac{d}{dt} \frac{\sigma_{\text{DW}}}{\lambda}, \quad (19)$$

which gives  $\lambda(t) \approx t^n$  with  $n = 1/3$ .

In conclusion, when faceting occurs we expect  $n = 1/3$  if dynamics can be characterized by a single length scale,  $\lambda$ . This result is in agreement with our formal derivation using the phase diffusion approach, but it is interesting to focus on the hypothesis of a single length scale. According to our approach [13], the periodic pattern is unstable against long-wave fluctuations whatever is its symmetry. However, when the current has a square symmetry [15] numerical simulations show a very irregular pattern which is characterized by two types of domain walls, therefore by two length scales. In poor words, one length scale is the length scale appearing in a perfectly periodic pattern, while the second length scale measures the size of ordered regions, i.e. the distance between defects. According to Refs. [15, 16] the structure would be metastable in the absence of such defects and the coarsening may be slowed, giving  $n = 1/4$  instead that  $n = 1/3$ . While our results contradict the metastable character of the periodic array, we cannot exclude that a *real* disordered pattern has a slower coarsening. A similar question seems to arise for rectangular symmetry. We refer the reader to [13] for a more detailed comparison with the literature.

#### IV. ELASTICITY

In the previous Section we have considered a growth phenomenon where coarsening is a pure nonequilibrium effect: if we switch off the flux coarsening stops and the surface relax towards the equilibrium state, corresponding to a flat surface plus thermal roughening (even if this relaxation may take a very long time). In fact, the destabilizing term in the evolution equation, the current  $\mathbf{j}$ , is proportional to the flux [17]. Furthermore, even if dynamics is driven by the minimization of a suitable functional  $\mathcal{F}$ , this pseudo free energy is a non equilibrium functional, whose form is completely different from the true free energy driving the relaxation towards equilibrium.

In this Section we are going to consider a problem which is apparently similar, but whose phenomenology and theoretical description are fairly different. The reason for that is *elasticity*, which comes into play when a solid is grown epitaxially on top of a substrate of different material. It is easy to understand what that means, because the “epitaxial constraint”, forcing to growth an adsorbate with a lattice constant imposed by the substrate has an effect similar to squeeze (or to stretch) a solid. Therefore, the system tries to reduce stress. This may be done either *breaking* the epitaxial constraint or not. The former case means that dislocations (i.e. defects breaking the translational invariance) form. At the end dislocations always form, but we are rather interested to the latter case, when epitaxy is maintained. In this case, surface modulations form giving rise to the so-called Asaro-Tiller-Grinfeld (ATG) instability [18]. This is the primary instability leading to quantum dot formation, see images (d1-d4) in Fig. 1.

The typical phenomenology of a process of heteroepitaxial growth includes the formation of a wetting layer, its destabilization just described, then the formation of islands. As a matter of fact, most of the interest towards these systems is related to their potential use as quantum dots, whose distribution should be as uniform as possible. In practice deposition is stopped after a while and the system is annealed waiting for its stabilization. This after-growth dynamics is much longer than the growth process itself and coarsening is expected to play a major role, with islands exchanging atoms to relax their energy.

This process closely resembles Ostwald ripening, where the average size of an ensemble of islands/clusters increases in time, driven by the Gibbs-Thomson effect [19]. Let’s spend a few words on this phenomenon, assuming that  $d$ -dimensional clusters exchange matter in a  $d$ -dimensional space because atoms detach/attach from clusters and diffuse from a high density to a low density region. The equilibrium density of atoms in proximity of a cluster of radius  $R$  has a curvature dependent contribution proportional to  $1/R$  (Gibbs-Thomson effect), so there will be a net current  $J$  from a smaller cluster to a larger cluster which reinforces their asymmetry in size and leads to an instability. Since the current is proportional to the density difference ( $\sim R^{-1}$ ) and inversely proportional to the distance between clusters ( $\sim R$ ),  $J \sim R^{-2}$ . If a cluster of size  $R$  is depleted by a current  $J \sim R^{-2}$ , it takes a time of order  $R^3$  to disappear, so we expect the typical size of survived clusters at time  $t$  is  $R \sim t^{1/3}$ .

This picture certainly cannot be applied to the heteroepitaxial case under study, and there is no simple picture or simple analytical treatment we can propose. This is due to two reasons: firstly, the system is intrinsically complicated,



with different energy terms which are all relevant: elastic stress, surface energy, and wetting interaction with the substrate; secondly, there are several (control) parameters which strongly affect the dynamics: the temperature, which controls surface diffusion, nucleation, intermixing; the misfit between substrate and adsorbate, which controls the strength of the elastic instability; the quantity of deposited material: the system first wets the substrate, then forms undulations and coherent dots, finally forms dislocations.

A good example of experimental overview is Ref. [20], where authors study the annealing of Ge islands on Si(100). With increasing  $T$ , they pass from observing a final stationary state to a coarsening process to an intermixing process between Ge and Si. And limiting ourselves to the coarsening regime, observed at  $T \approx 600^\circ\text{C}$ , island shape changes with size. Changes of shape during coarsening have also been observed in precipitates in solids [21] and leads to multimodal distributions of the size of aggregates. This fact clearly makes the theoretical analysis more difficult.

From the point of view of this paper the main question is whether the final state of the evolution is a periodic array of islands/dots or if we should expect an ongoing coarsening. The question has energetic and kinetic aspects and even from a purely energetic point of view it is not trivial at all. In fact the minimization of the full energy is practically not feasible, because of the many terms entering in the energy, the nonlocal character of elastic interactions, and the variety of periodic arrays that should be taken into account in the minimization. Nonetheless, some attempts have been done, e.g., by V.A. Shchukin and collaborators [22–24], finding that arrays are at least metastable. Experimental data in agreement with this result and providing a stable or metastable bimodal distribution (pyramids and domes) have been found by Medeiros-Ribeiro and collaborators [25]. However, this picture has been opposed in Refs. [26, 27], where authors dispute the idea that different types of dots are in equilibrium with each other. Rather, they suggest that a subtle interplay between thermodynamics and kinetics is responsible of the dynamics of the system and the size distribution is not steady but it continues to evolve through an anomalous coarsening involving a change of shape of dots.

It follows that it is crucial to take into account kinetics through an evolution equation, but we should add that the resulting picture is strongly dependent on the basic ingredients used to build up the model. For example, linear elasticity and a non singular wetting potential have provided [28] a steady final state, but a different wetting interaction and its effect on stress make islands unstable and coarsening is restored [29]. A careful approach has been undertaken by J.-N. Agra and collaborators, who have included nonlinear elastic effects [30, 31] and anisotropy effects [32]. According to their results the isotropic system displays interrupted coarsening, while anisotropy changes islands' shape (as expected) and arrest coarsening. This picture of interrupted coarsening is also found experimentally [32] on SiGe/Si, see Figs. 1d.

## V. EROSION

So far we have discussed coarsening phenomena having two common features: they are driven by thermally activated elementary processes and they occur during a growth process (or during the annealing following a growth process). This Section differs in both aspects, since the morphology is driven by bombarding and eroding the surface with an energetic flux of ions. Each ion penetrates the surface and releases its energy in the surrounding environment, which allows to kick atoms out.[52]

In Fig. 1(e1-e4) we reproduce some STM topographs by Martin Engler et al. [6] showing a Si(001) surface after  $\text{Kr}^+$  bombardment: the initially flat surface is destabilized and an array of ripples appears with an increasing wavelength. Such a regular morphology (attested by height profiles, see [6]) is not obvious and we might expect that eroded surfaces undergo a kinetic roughening process, as it actually happens in other cases [33]. It is hard to evaluate a priori the relevance of noise and in the literature there are analyses of sputter erosion based on stochastic equations like the anisotropic Kardar-Parisi-Zhang equation [34]. However, most studies are focused on deterministic equations where roughening is the result of an instability. We will limit here to deterministic processes.

The primary question when facing an instability concerns its origin: why does it rise? The first answer was proposed by Bradley and Harper [35] who suggested that erosion velocity might depend on the curvature, being larger for a positive curvature. This fact alone leads to an evolution equation like  $\partial_t h = -\nu \nabla^2 h$ , which displays an instability. In subsequent years other mechanisms and linear theories have been proposed, evoking mass redistribution [36], ion induced flows [37], and so on. These few words just to make it clear that physical processes at the origin of the instability are not fully understood, also because they may depend on the material and on the erosion conditions.

A linear theory is also able to address the size and the orientation of the emergent structure and different answers can be obtained to questions about ripple rotation and the effective unstable character of the flat surface with varying the incidence angle of the beam. For example, recent experimental answers to these issues have appeared for erosion patterns on Ge(100) [38] and Si(001) [6]. In these papers authors do not observe ripple rotation and they don't even observe ripple formation for normal or quasi normal incidence. Instead, for oblique incidence they record coarsening processes, see Figs. 1e for Si. Coarsening is described as a nonlocal process, due to the reflection of ions from the

downwind face towards the upwind face [39].

A different coarsening picture emerges from other erosion experiments on Si [40–42], where authors report to observe interrupted coarsening. It is possible, as the authors say, that metal impurities and silicide formation could influence the pattern morphology and its dynamical evolution. Their picture of interrupted coarsening is based on an analytical model which is worth discussing,

$$\frac{\partial h}{\partial t} = -\nu \nabla^2 h - \mathcal{K} \nabla^4 h + \lambda_1 (\nabla h)^2 - \lambda_2 \nabla^2 (\nabla h)^2. \quad (20)$$

The linear part is standard: the  $\nu$ -term is responsible for the instability and the  $\mathcal{K}$ -term heals the instability at short length scales. Their balance produces an initial pattern of wavelength  $\lambda_c = 2\pi(2\mathcal{K}/\nu)^{1/2}$ . The nonlinear part is composed of a conserved term ( $\lambda_2$ ) and a nonconserved one ( $\lambda_1$ ). Without the latter term, the above equation becomes the conserved Kuramoto-Sivashinsky equation,  $\partial_t h = -\nabla^2(\nu h + \mathcal{K} \nabla^2 h + \lambda_2 (\nabla h)^2)$ , which is known to display perpetual coarsening [43, 44]. In the opposite limit,  $\lambda_2 = 0$ , we get the standard Kuramoto-Sivashinsky equation, which is known to display spatio-temporal chaos with a cellular structure of order  $\lambda_c$ . It is not trivial that their combination may produce interrupted coarsening and it would be interesting (but fairly complicated in 2D) to study Eq. (20) with the phase diffusion approach discussed in Sec. III.

## VI. FINAL CONSIDERATIONS

The first general remark is that dynamics may be driven by some free energy. It may be a real free energy, see Sec. IV, or a pseudo free energy, see Sec. III. It is not granted that dynamics allows to attain the ground state and the interruption of coarsening may be determined by the trapping in some metastable state. The presence of elasticity makes the problem so complicated it is not even possible to know what pattern minimizes the energy, especially in two spatial dimensions, which is the only physically relevant case. Furthermore, simple models of the ATG instability produce finite time singularities which need to be regularized [45].

In the kinetic-driven case, Sec. III, the existence of a pseudo free energy is not really relevant. For example, the one-dimensional problem describing the in-phase meandering of a vicinal surface is studied by Eq. (8) which cannot always be put into a variational form. In spite of this, its analysis by the phase diffusion equation can be performed giving a very general criterion for the existence of coarsening: the wavelength of periodic steady states is an increasing function of their amplitude. The same approach can be employed in 2D, even if such simple criterion seems to be applicable only for small amplitude structures, in the general case the coarsening criterion being the negativity of a suitable diffusion coefficient.

Apart from the exact coarsening criterion, an important feature of the kinetic-driven case is that interrupted coarsening is accompanied by a diverging amplitude, the final state as described by Eqs. (8,10) not being stationary. This scenario corresponds to what is really observed, e.g., in the growth of Pt/Pt(111), where wedding cakes of increasing height and constant lateral size are finally obtained, see Figs. 1c. This system seems to be the experimental realization of the simple Zeno model introduced long time ago [46, 47].

In the other cases studied here, interrupted coarsening means attaining a final structure which is finite in wavelength *and* amplitude, even if it may not correspond to the minimal energy state. In general terms, it seems that at least three mechanisms of interrupted coarsening exist: the simplest one occurs when dynamics is driven by a free energy which is minimized by a structure of finite size; the second one corresponds to the kinetic-driven case of our Sec. III, where the final state has a diverging amplitude; the third one appears in the erosion problem, Sec. V, where the interruption seems to be the result of a competition between a perpetual coarsening dynamics and a constant wavelength scenario. This classification does not pretend to go beyond the problems studied here. For example, it is known that quenched disorder [48] or the existence of stirring in a binary fluid may also lead to coarsening interruption or to its sharp slowdown.

When a perpetual coarsening process occurs, it is important to study its growth law, usually a power law one. The phase diffusion approach allows to determine the coarsening exponent  $n$ , but our results for the 2D growth law on a high symmetry surface do not agree with other findings, especially numerics, concerning square symmetry. A possible explanation is that the emerging square pattern seems to be fairly disordered, so that the time scale derived from a periodic array might not be the appropriate one.

The topics discussed in this paper have the nice feature to be characterized by a strong link among theory, simulations and experiments. On the one hand, the more a phenomenon is widespread the more it is worth studying. On the other hand, it would be important to have an agreed “model system” so as to allow a quantitative comparison between theory/simulations and experiments. Coarsening dynamics are widespread in each of the three subfields discussed here, but it seems to us that some efforts are needed for the energetic and the athermal cases in order to

identify a *simple* theoretical model, or a *simple* experimental system, or both. Nobody can assure this is possible, of course.

### Acknowledgements

I acknowledge Isabelle Berbezier for the experimental images (d1-d4) in Fig. 1. I profited a lot from discussions and from the critical reading of the manuscript of several persons: Jean-Noël Aqua, Claudia Innocenti, Thomas Michely, Chaouqi Misbah, Matteo Nicoli, and Jacques Villain.

- 
- [1] J. Stewart and N. Goldenfeld, Phys. Rev. A **46**, 6505 (1992).
  - [2] F. Liu and H. Metiu, Phys. Rev. B **48**, 5808 (1993).
  - [3] J.-K. Zuo and J. F. Wendelken, Phys. Rev. Lett. **78**, 2791 (1997).
  - [4] N. Néel, T. Maroutian, L. Douillard, and H.-J. Ernst, Journal of Physics: Condensed Matter **15**, S3227 (2003).
  - [5] M. Kalf, P. Šmilauer, G. Comsa, and T. Michely, Surface science **426**, L447 (1999).
  - [6] M. Engler, S. Macko, F. Frost, and T. Michely, Phys. Rev. B **89**, 245412 (2014).
  - [7] S. Paulin, F. Gillet, O. Pierre-Louis, and C. Misbah, Phys. Rev. Lett. **86**, 5538 (2001).
  - [8] C. Misbah, O. Pierre-Louis, and Y. Saito, Rev. Mod. Phys. **82**, 981 (2010).
  - [9] G. B. Whitham, *Linear and nonlinear waves*, volume 42, John Wiley & Sons, 2011.
  - [10] P. Politi and C. Misbah, Phys. Rev. E **73**, 036133 (2006).
  - [11] G. Danker, O. Pierre-Louis, K. Kassner, and C. Misbah, Phys. Rev. E **68**, 020601 (2003).
  - [12] S. Biagi, C. Misbah, and P. Politi, Phys. Rev. Lett. **109**, 096101 (2012).
  - [13] S. Biagi, C. Misbah, and P. Politi, Phys. Rev. E **89**, 062114 (2014).
  - [14] L. Golubovic, A. Levandovsky, and D. Moldovan, East Asian Journal on Applied Mathematics **1**, 297 (2011).
  - [15] A. Levandovsky and L. Golubović, Phys. Rev. B **69**, 241402 (2004).
  - [16] M. Siegert, Phys. Rev. Lett. **81**, 5481 (1998).
  - [17] P. Politi, Comptes Rendus Physique **7**, 272 (2006), High power fiber lasers and amplifiers Lasers et amplificateurs à fibre de puissance.
  - [18] P. Politi, G. Grenet, A. Marty, A. Ponchet, and J. Villain, Physics Reports **324**, 271 (2000).
  - [19] Y. Saito, *Statistical physics of crystal growth*, volume 2, World Scientific, 1996.
  - [20] T. Kamins, G. Medeiros-Ribeiro, D. Ohlberg, and R. S. Williams, Journal of applied physics **85**, 1159 (1999).
  - [21] U. Dahmen, S. Xiao, S. Paciornik, E. Johnson, and A. Johansen, Phys. Rev. Lett. **78**, 471 (1997).
  - [22] V. A. Shchukin, N. N. Ledentsov, P. S. Kop'ev, and D. Bimberg, Phys. Rev. Lett. **75**, 2968 (1995).
  - [23] V. A. Shchukin and D. Bimberg, Rev. Mod. Phys. **71**, 1125 (1999).
  - [24] V. A. Shchukin, D. Bimberg, T. P. Munt, and D. E. Jesson, Phys. Rev. Lett. **90**, 076102 (2003).
  - [25] G. Medeiros-Ribeiro, A. M. Bratkovski, T. I. Kamins, D. A. A. Ohlberg, and R. S. Williams, Science **279**, 353 (1998).
  - [26] F. M. Ross, J. Tersoff, and R. M. Tromp, Phys. Rev. Lett. **80**, 984 (1998).
  - [27] A. Rastelli, M. Stoffel, J. Tersoff, G. S. Kar, and O. G. Schmidt, Phys. Rev. Lett. **95**, 026103 (2005).
  - [28] W. T. Tekalign and B. Spencer, Journal of applied physics **96**, 5505 (2004).
  - [29] M. S. Levine, A. A. Golovin, S. H. Davis, and P. W. Voorhees, Phys. Rev. B **75**, 205312 (2007).
  - [30] J.-N. Aqua, T. Frisch, and A. Verga, Phys. Rev. B **76**, 165319 (2007).
  - [31] J.-N. Aqua, I. Berbezier, L. Favre, T. Frisch, and A. Ronda, Physics Reports **522**, 59 (2013), Growth and self-organization of SiGe nanostructures.
  - [32] J.-N. Aqua, A. Gouyé, A. Ronda, T. Frisch, and I. Berbezier, Phys. Rev. Lett. **110**, 096101 (2013).
  - [33] E. A. Eklund, R. Bruinsma, J. Rudnick, and R. S. Williams, Phys. Rev. Lett. **67**, 1759 (1991).
  - [34] R. Cuerno and A.-L. Barabási, Phys. Rev. Lett. **74**, 4746 (1995).
  - [35] R. M. Bradley and J. M. E. Harper, Journal of Vacuum Science & Technology A **6**, 2390 (1988).
  - [36] S. A. Norris, M. P. Brenner, and M. J. Aziz, Journal of Physics: Condensed Matter **21**, 224017 (2009).
  - [37] R. Cuerno, M. Castro, J. Muñoz-García, R. Gago, and L. Vázquez, Nuclear Instruments and Methods in Physics Research Section B: Beam Interactions with Materials and Atoms **269**, 894 (2011), Atomic Collisions in Solids Proceedings of the 24th International Conference on Atomic Collisions in Solids (ICACS-24).
  - [38] M. Teichmann, J. Lorbeer, B. Ziberi, F. Frost, and B. Rauschenbach, New Journal of Physics **15**, 103029 (2013).
  - [39] W. Hauffe, physica status solidi (a) **35**, K93 (1976).
  - [40] J. Muñoz García, R. Gago, L. Vázquez, J. A. Sánchez-García, and R. Cuerno, Phys. Rev. Lett. **104**, 026101 (2010).
  - [41] J. M. noz García et al., Journal of Physics: Condensed Matter **24**, 375302 (2012).
  - [42] J. Muñoz-García et al., Materials Science and Engineering: R: Reports **86**, 1 (2014).
  - [43] T. Frisch and A. Verga, Phys. Rev. Lett. **96**, 166104 (2006).
  - [44] M. Nicoli, C. Misbah, and P. Politi, Phys. Rev. E **87**, 063302 (2013).
  - [45] K. Kassner, C. Misbah, J. Müller, J. Kappey, and P. Kohlert, Phys. Rev. E **63**, 036117 (2001).

- [46] I. Elkinani and J. Villain, *Journal de Physique I* **4**, 949 (1994).
- [47] P. Politi and J. Villain, *Phys. Rev. B* **54**, 5114 (1996).
- [48] F. Corberi, Coarsening in inhomogeneous systems, This Issue.
- [49] It is called vicinal because its Miller indexes are close (vicinal) to those of a high symmetry surface.
- [50] In this homoepitaxial context, elastic interactions between steps or adatoms do not imply long range interactions.
- [51] In  $D = 2$ , the criterion because coarsening occurs is a generalized version of the condition  $\partial_A \lambda > 0$ , where the amplitude  $A$  of the steady pattern is replaced by a more complicated quantity. This quantity reduces to  $A$  for small  $A$ .
- [52] Sputtered atoms can then deposit onto another surface. We are not interested here in this amorphous growth process, but in the erosion process.